9852 *Inorg. Chem.* **2010**, *49*, 9852–9862
DOI: 10.1021/ic101128w

Inorganic Chemistry
Article

High-Throughput Aided Synthesis of the Porous Metal−Organic Framework-Type Aluminum Pyromellitate, MIL-121, with Extra Carboxylic Acid Functionalization

Christophe Volkringer,[†] Thierry Loiseau,*[,†] Nathalie Guillou,[†] Gérard Férey,[†,‡] Mohamed Haouas,[§] Francis Taulelle,[§] Erik Elkaim,[∥] and Norbert Stock[⊥]

[†]*Porous Solids Group, Institut Lavoisier de Versailles,* [‡]*Institut Universitaire de France, and* [§]*Tectospin, Institut Lavoisier de Versailles, Université de Versailles Saint Quentin en Yvelines, 45, avenue des Etats-Unis, 78035 Versailles, France,* [∥]*Soleil Synchrotron, L'Orme des Merisiers, Saint-Aubin, BP 48, 91192 Gif-sur-Yvette cedex, France, and* [⊥]*Institute of Inorganic Chemistry, Christian-Albrechts-University, Max-Eyth-Strasse 2, 24118 Kiel, Germany*

Received June 4, 2010

A new porous metal−organic framework (MOF)-type aluminum pyromellitate (MIL-121 or Al(OH)[H_2btec]·(guest), (guest = H_2O, H_4btec = pyromellitic acid) has been isolated by using a high-throughput synthesis method under hydrothermal conditions. Its structure was determined from powder X-ray diffraction analysis using synchrotron radiation (Soleil, France) and exhibits a network closely related to that of the MIL-53 series. It is a three-dimensional (3D) framework containing one-dimensional (1D) channels delimited by infinite trans-connected aluminum-centered octahedra $AlO_4(OH)_2$ linked through the pyromellitate ligand. Here the organic ligand acts as tetradendate linker via two of the carboxylate groups. The two others remain non-bonded in their protonated form, and this constitutes a rare case of the occurrence of both bonding and non-bonding organic functionalities of the MOF family. The non-coordinated −COOH groups points toward the channels to get them an open form configuration. Within the tunnels are located unreacted pyromellitic acid and water species, which are evacuated upon heating, and a porous MIL-121 phase is obtained with a Brunauer−Emmett−Teller (BET) surface area of 162 $m^2\ g^{-1}$. MIL-121 has been characterized by IR, thermogravimetry (TG) analyses, and solid state NMR spectroscopy employing a couple of two-dimensional (2D) techniques such as ^{1}H-^{1}H SQ-DQ BABA, ^{1}H-^{1}H SQ-SQ RFDR, ^{27}Al{^{1}H} CPHETCOR and ^{27}Al MQMAS.

Introduction

Since the pioneering work of Hoskins and Robson,[1,2] the search for new coordination polymers and metal−organic frameworks (MOFs) has grown exponentially. This interest is mostly due to the occurrence of the wide variety and beautiful architectures, promising applications, and unprecedented properties.[3−7] These compounds are synthesized from the condensation of metallic cations into discrete or infinite inorganic moieties connected to each other via organic molecules. Usually, aromatic carboxylates are preferred to other ligands because they generate robust three-dimensional (3D) frameworks with interesting porous properties and large aperture windows (greater than those observed in zeolites). Another advantage of MOFs over the purely inorganic compounds is the possibility to integrate chemical functionalities on the organic part. This strategy can be a way to access more efficient compounds for more specific applications.

The functionalization of the organic linker can be achieved with specific moieties (−NH_2, −Br, −Cl, −CH_3) attached to the ligand precursor before the reaction or with covalent post synthetic modification (PSM) of these branched groups.[8,9] For instance, the most popular functionalized ligand for MOF synthesis and covalent PSM is the aminoterephthalic acid, since it leads to many open-framework structures with a large choice of covalent PSM.[8,10−21] Another promising

*To whom correspondence should be addressed. E-mail: thierry.loiseau@ensc-lille.fr. Phone: (33) 3 20 33 64 34. Fax: (33) 3 20 43 48 95. Present address: Unité de Catalyse et Chimie du Solide−UMR CNRS 8181, USTL-ENSCL, Université de Lille, 59652 Villeneuve d'Ascq, France.

(1) Hoskins, B. F.; Robson, R. *J. Am. Chem. Soc.* **1989**, *111*, 5962.
(2) Robson, R. *Dalton Trans.* **2008**, 5113.
(3) Férey, G. *Chem. Soc. Rev.* **2008**, *37*, 191.
(4) Kitagawa, S.; Kitaura, R.; Noro, S.-I. *Angew. Chem., Int. Ed.* **2004**, *43*, 2334.
(5) Yaghi, O. M.; O'Keeffe, M.; Ockwig, N. W.; Chae, H. K.; Eddaoudi, M.; Kim, J. *Nature* **2003**, *423*, 705.
(6) Janiak, C. *Dalton Trans.* **2003**, 2781.
(7) Czaja, A. U.; Trukhan, N.; Müller, U. *Chem. Soc. Rev.* **2009**, *38*, 1284.
(8) Wang, Z.; Cohen, S. M. *Chem. Soc. Rev.* **2009**, *38*, 1315.
(9) Fischer, R. A.; Wöll, C. *Angew. Chem., Int. Ed.* **2008**, *48*, 8164.
(10) Roswell, J. L. C.; Yaghi, O. M. *J. Am. Chem. Soc.* **2006**, *128*, 1304.
(11) Wang, Z.; Cohen, S. M. *J. Am. Chem. Soc.* **2007**, *129*, 12368.
(12) Costa, J. S.; Gamez, P.; Black, C. A.; Roubeau, O.; Teat, S. J.; Reedijk, J. *Eur. J. Inorg. Chem.* **2008**, 1551.
(13) Dugan, E.; Wang, Z.; Okamura, M.; Medina, A.; Cohen, S. M. *Chem. Commun.* **2008**, 3366.

 Published on Web 10/05/2010

function for MOF-type metal carboxylates might be the occurrence of free carboxylic acid.[22] But this choice needs a perfect control of the reaction conditions to generate at the same time and on the same ligand, free −COOH and coordinated −COO carboxylate functions. To our knowledge, very few compounds have been described having a non-coordinated −COOH group after synthesis, including the divalent copper binicotinate,[23] iron,[24,25] and gallium[26] pyromellitates, which are unfortunately non-porous. In our study of the reactivity of trivalent cations, we focused our efforts in the elaboration of aluminum-based MOFs and very recently different teams described the synthesis and the properties of functionalized aluminum terephthalates of MIL-53 type. These works showed very interesting and promising properties for gas storage,[17,27] gas separation,[28] and catalysis.[18,29]

This contribution deals with the synthesis of a MIL-53(Al) analogue, containing two extra free carboxylic acid functions per ligand with interesting porosity. This new MOF, called MIL-121(Al) (Al(OH)[H_2btec]·(guest) (guest = H_2O, H_4btec) was obtained with the pyromellitic acid (1,2,4,5-benzenetetracarboxylic acid or H_4btec). It results from a systematic investigation of the chemical system $Al(NO_3)_3 \cdot 9H_2O/H_4$btec/$H_2O$/NaOH applying high-throughput synthesis methods.[19,21,30−32] This is the third member of the aluminum pyromellitate series, which cocrystallized with two others, MIL-118[33] and MIL-120.[34] We show that the starting pH value is critical for controlling at the same time the number of free carboxylic acid functions of the aromatic ligand and the carboxylate groups coordinated to aluminum involved in infinite inorganic chains. The structure of MIL-121(Al) is analyzed by powder X-ray diffraction (XRD) using synchrotron radiation and solid-state NMR (^{27}Al, ^{13}C, ^{1}H). The porosity of the activated sample has been also characterized by nitrogen adsorption.

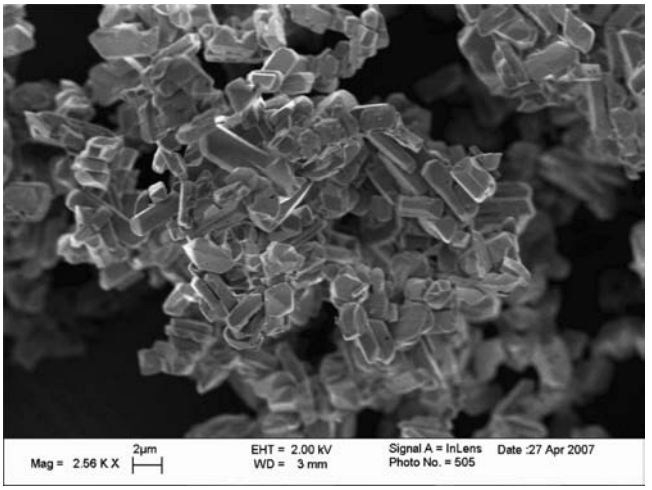

Figure 1. SEM image of the as-synthesized aluminum pyromellitate (MIL-121_as) showing agglomerates of parallepiped shape crystals.

Experimental Section

Synthesis. The title compound MIL-121 was hydrothermally synthesized from a mixture of aluminum nitrate nonahydrate ($Al(NO_3)_3 \cdot 9H_2O$, Carlo Erba, 99+%), pyromellitic acid (1,2,4,5-benzenetetracarboxylic acid, noted H_4btec, $C_6H_2(CO_2H)_4$, Aldrich, 96%) and deionized water. The following typical composition of 1.2 g of $Al(NO_3)_3 \cdot 9H_2O$ (3.2 mmol), 0.4 g of H_4btec (1.6 mmol), 5 mL of H_2O (278 mmol) was placed in a Teflon cell, then in a Parr-type steel autoclave (23 mL), and heated in an oven for 24 h at 210 °C. The starting pH value was 1.41 and 0.26 at the end of the reaction. It resulted in a white powdered product (MIL-121_as), which was filtered off, washed with deionized water, and dried at room temperature. The scanning electron microscopy (SEM) examination (LEO 1530) showed that the MIL-121_as compound consists of tiny parallelepiped-like crystallites of 1−4 μm size (Figure 1). In fact, two other aluminum pyromellitates, MIL-118A[33] and MIL-120[34] have been previously isolated, and high-throughput combinatorial chemistry procedures were used to identify the domains of existence of the three distinct phases. More details are given in the sections below.

The empty pore MIL-121 compound has been obtained by following a heating process at 380 °C for 5 h and referred to MIL-121_ht.

High-Throughput Experiments. The investigation of the reaction system Al−H_4btec-H_2O was performed under hydrothermal reaction conditions by employing a multiclave containing 48 Teflon reactors of 0.25 mL each.[30] With such a setup, it is possible to explore different molar compositions in one reaction batch and thus to quickly discover and optimize the right conditions of crystallization of a given phase. This is particularly efficient for complex chemical systems with different phases. The high throughput technique was applied for the study of the reaction of the pyromellitate ligand with aluminum in water (heating time: 24 h at 180 °C), and this revealed the crystallization domains of the three different phases occurring in this chemical system. The high-throughput X-ray analyses were performed in transmission geometry using a STOE HT powder diffractometer equipped with a *xy*-stage and a linear position sensitive detector (PSD) system.

Powder XRD Analysis. The structure of MIL-121 was determined by means of the powder XRD technique using synchrotron

(14) Ingelson, M. J.; Barrio, J. P.; Guilbaud, J. B.; Khimyak, Y. Z.; Rosseinsky, M. J. *Chem. Commun.* **2008**, 2680.
(15) Tanabe, K. K.; Wang, Z.; Cohen, S. M. *J. Am. Chem. Soc.* **2008**, *130*, 8508.
(16) Wang, Z.; Cohen, S. M. *Angew. Chem., Int. Ed.* **2008**, *47*, 4699.
(17) Ahnfeldt, T.; Gunzelmann, D.; Loiseau, T.; Hirsemann, D.; Senker, J.; Férey, G.; Stock, N. *Inorg. Chem.* **2009**, *48*, 3057.
(18) Gascon, J.; Aktay, U.; Hernandez-Alonso, M. D.; van Klink, G. P. M.; Kapteijn, F. *J. Catal.* **2009**, 261.
(19) Ahnfeldt, T.; Guillou, N.; Gunzelmann, D.; Margiolaki, I.; Loiseau, T.; Férey, G.; Senker, J.; Stock *Angew. Chem., Int. Ed.* **2009**, *48*, 5163.
(20) Wang, Z.; Tanabe, K. K.; Cohen, S. M. *Inorg. Chem.* **2009**, *48*, 296.
(21) Bauer, S.; Serre, C.; Devic, T.; Horcajada, P.; Marrot, J.; Férey, G.; Stock, N. *Inorg. Chem.* **2008**, *47*, 7568.
(22) Gadzikwa, T.; Farha, O. K.; Mulfort, K. L.; Hupp, J. T.; Nguyen, S. T. *Chem. Commun.* **2009**, 3720.
(23) Custelcean, R.; Gorbunova, M. G. *J. Am. Chem. Soc.* **2005**, *127*, 16362.
(24) Chu, D.-Q.; Pan, C.-L.; Wang, L.-M.; Xu, J.-Q. *Mendeleev Commun.* **2002**, 207.
(25) Sanselme, M.; Grenèche, J.-M.; Riou-Cavellec, M.; Férey, G. *Solid State Sci.* **2004**, *6*, 853.
(26) Loiseau, T.; Muguerra, H.; Haouas, M.; Taulelle, F.; Férey, G. *Solid State Sci.* **2005**, *7*, 603.
(27) Himst, D.; Wallacher, D.; Hartmann, M. *Angew. Chem., Int. Ed.* **2009**, *48*, 4639.
(28) Couck, S.; Denayer, J. F.; Baron, G. V.; Rémy, T.; Gascon, J.; Kapteijn, F. *J. Am. Chem. Soc.* **2009**, *131*, 6326.
(29) Meilikhov, M.; Yusenko, K.; Fischer, R. A. *J. Am. Chem. Soc.* **2009**, *131*, 9644.
(30) Stock, N.; Bein, T. *Angew. Chem.* **2004**, *116*, 767.
(31) Sonnauer, A.; Hoffmann, F.; Froba, M.; Kienle, L.; Duppel, V.; Thommes, M.; Serre, C.; Férey, G.; Stock, N. *Angew. Chem., Int. Ed.* **2009**, *48*, 3791.
(32) Stock, N. *Microporous Mesoporous Mater.* **2010**, *129*, 287.
(33) Volkringer, C.; Loiseau, T.; Guillou, N.; Férey, G.; Haouas, M.; Taulelle, F.; Audebrand, N.; Margiolaki, I.; Popov, D.; Burghammer, M.; Riekel, C. *Cryst. Growth. Des.* **2009**, *9*, 2927.
(34) Volkringer, C.; Loiseau, T.; Haouas, M.; Taulelle, F.; Popov, D.; Burghammer, M.; Riekel, C.; Zlotea, C.; Cuevas, F.; Latroche, M.; Phanon, D.; Knöfelv, C.; Llewellyn, P. L.; Férey, G. *Chem. Mater.* **2009**, *21*, 5783.

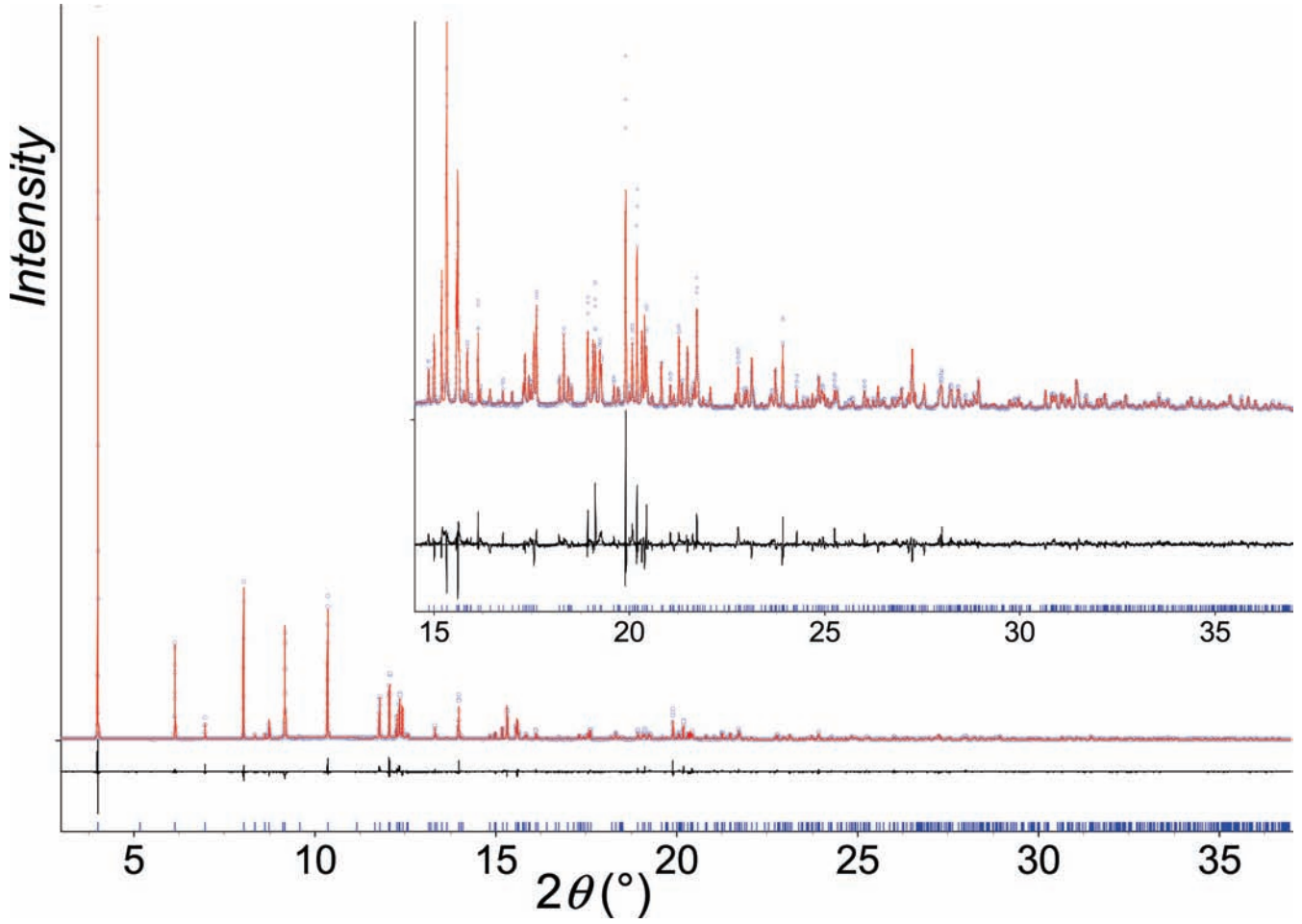

Figure 2. Final Rietveld plot of the MIL-121_as compound (X-ray powder data from station CRISTAL at Soleil, $\lambda = 0.7285$ Å, room temperature). Observed data are shown by circles; the calculated pattern is displayed by the red solid line; the lower black curve is a plot of the difference, observed minus calculated.

radiation at station CRISTAL from the Soleil Source (Gif sur Yvette, France). A monochromatic beam of wavelength 0.7285 Å was extracted from the undulator beam using a double crystal Si(111) monochromator. The sample was loaded in a 0.7 mm diameter glass capillary, which was mounted on a two circle diffractometer equipped with a 13 crystals multianalyzer. With this setup, it took less than 2 h in continuous scanning mode to collect a high angular resolution diagram. The experimental data files are obtained from the precise superposition and addition of the 13 channels data.

The XRD powder pattern has been indexed and refined by using the TOPAS 4.2[35] suite. A monoclinic unit cell was found unambiguously (LSI-Indexing method) with satisfactory figure of merit ($M_{20} = 276$) and systematic extinctions consistent with $C2/c$ or Cc space groups. The centrosymetric space group was chosen and calculations were performed with the EXPO[36] package, using EXTRA for extracting integrated intensities and SIR*97* for direct methods structure solution. A list of 509 reflections was extracted in the angular range $1-37°(2\theta)$. According to the degree of diffraction overlap, 56.87% of these reflections were statistically considered as independent and all atoms of the hybrid framework were found unambiguously from the E-map with the highest figure of merit. The corresponding atomic coordinates were then used as a starting model in the Rietveld refinement. The occluded water molecule as well as carboxylic functions of the occluded organic moiety were seen in difference Fourier maps, but it was impossible to distinguish C atoms of the benzene ring. The free organic molecule was then treated as a rigid body, and it was localized by using a direct space approach based on simulated annealing. At the final stage, Rietveld refinement involved the following structural parameters: 30 atomic coordinates, 3 rotation parameters for the free pyromellitate as well as 6 distances and 2 torsion angles in the rigid body, 4 thermal factors, 2 occupancy factors, and 1 scale factor. The anisotropic line broadening effect was corrected by using spherical harmonics series, and soft restraints were maintained on the organic ligand. The final Rietveld plot (Figure 2) corresponds to satisfactory model indicators and profile factors (see Table 1). From this analysis, a chemical formula of MIL-121 can be proposed with a content of 0.27 for free pyromellitic acid and 0.19 trapped water per Al(OH)[$C_{10}O_8H_4$] unit.

Variable-temperature in situ X-ray powder patterns were collected under static air on a Siemens D5000 diffractometer ($\theta-\theta$ mode) using cobalt radiation equipped with an Anton Parr HTK16 high temperature device and M Braun linear position sensitive detector (PSD). Each powder pattern was recorded in the range $8-32°$ (2θ) (at intervals of 20 °C up to 580 °C) with a 2 s/step scan, corresponding to an approximate duration of 1 h. The temperature ramp between two patterns was 5 °C.min^{-1}.

Thermogravimetric Analyses. The thermogravimetric (TG) experiments were carried out on a TA Instruments type 2050 thermoanalyzer under oxygen gas flow with a heating rate of 1 °C.min^{-1}.

(35) *Topas, General Profile and Structure Analysis Software for Powder Diffraction Data*, V4.2; Bruker AXS Ltd: Madison, WI, 2008.

(36) Altomare, A.; Burla, M. C.; Carrozzini, B.; Cascarano, G.; Giacovazzo, C.; Guagliardi, A.; Moliterni, A. G. G.; Polidori, G.; Rizzi, R. *J. Appl. Crystallogr.* **1999**, *32*, 339.

Table 1. Crystal Data and Structure Refinement for MIL-121

	MIL-121
chemical formula	$Al(OH)[C_{10}O_8H_4]\cdot xH_2O\cdot yC_{10}O_8H_6$[a]
formula weight (g/mol)	367.96
temperature (K)	296
wavelength (Å)	0.7285
symmetry	monoclinic
space group	$C2/c$
a (Å)	17.54483(8)
b (Å)	13.57813(8)
c (Å)	6.66420(4)
β (deg)	113.1956(5)
V (Å^3)	1459.25(2)
Z, calculated density	4, 1.524
2θ range (deg)	3.0 to 37.0
no. reflections	526
no. non hydrogen atoms	29
GoF	2.403
no. structural parameters	48
R_{wp}	0.110
R_p	0.081
R_{Bragg}	0.052

[a] With $x = 0.19(2)$ and $y = 0.269(2)$.

Surface Area Measurement. The porosity of MIL-121 was determinated from a gas sorption isotherm measurement in liquid nitrogen using a Micromeritics ASAP2010 apparatus. Before the sorption experiment, the sample was outgassed under primary vacuum (5 Pa) at 200 °C for 15 h.

Solid State NMR. All MAS NMR studies were carried out in the magic angle-spinning mode using a Bruker AVANCE 500 spectrometer at resonance frequencies of 500.13 MHz, 130.32 and 125.78 MHz for ^{1}H, ^{27}Al, and ^{13}C respectively. For all the experiments a standard 2.5 mm double-bearing Bruker MAS probe was used. ^{1}H MAS NMR spectra were recorded with a 2.5 mm MAS rotor system after a $\pi/4$ single-pulse excitation of 5.3 μs with repetition time of 4 s. Experiments were performed with a sample rotation frequency of 30 kHz. An average of 80 scans was collected for each sample. To observe correlation between ^{1}H nuclei, homonuclear dipolar recoupling back-to-back (BABA) sequence[37] was used in magic-angle spinning (MAS) with both frequency dimensions synchronized to the rotation frequency. The BABA sequence allows the recoupling of the dipolar interaction, which is averaged by MAS. Two-dimensional (2D) ^{1}H NMR radio frequency dipolar recoupling (RFDR) experiments were also carried out. The ^{1}H MAS BABA and RFDR were acquired in a phase sensitive mode using time proportional phase increment (TPPI) and states methods, respectively. A total of 128 increments, each with 128 or 32 scans were collected for ^{1}H MAS BABA or RFDR. A series of 32 presaturation scans at the beginning of each experiment were used to establish steady state magnetization. A repetition delay of 1 s was used in both experiments. ^{1}H→^{13}C CP MAS NMR spectrum was recorded with a spinning speed of 12.5 kHz. The contact times of the ^{1}H→^{13}C CP MAS NMR experiments was optimized as 5 ms, the recycle delay was 3.5 s, and the experiment was performed with an accumulation number of 14336. Values of the isotropic chemical shifts of ^{1}H, and ^{13}C are given with respect to TMS. ^{1}H decoupled ^{27}Al MAS NMR measurements were carried out with 2.5 mm MAS rotor system. Pulse length of the aluminum $\pi/12$ pulse was 6.4 μs, and repetition time for the experiments was 0.2 s. All spectra were collected at a spinning rate of 30 kHz. ^{1}H decoupling applied during the acquisition time was found to have some effect on the width of the peaks in the ^{27}Al spectrum. Chemical shifts were represented with reference to $Al(NO_3)_3$ peak at 0 ppm. The average number of scans collected for the experiments were about 4000 for the samples. The DMFIT software was used to fit the spectra and obtain the line characteristics (isotropic chemical shifts, quadrupolar coupling constants, and asymmetry parameters), and the percentage of each contribution.[38] ^{1}H→^{27}Al HETCOR NMR spectra have been obtained with contact times of 0.1−1.5 ms, and a recycle delay of 0.3 s. To improve the spin-lock efficiency of the quadrupolar ^{27}Al, the experiments have been performed in the "sudden passage regime" using a high spinning rate of 30 kHz, and a low RF field strength for the contact pulses (6−7 kHz for ^{27}Al). The 2D ^{1}H→^{27}Al HETCOR NMR spectra have been acquired with an evolution t_1 time period, after the first ^{27}Al excitation pulse, incremented to one rotor period (33.3 μs). Thirty-two t_1 increments were obtained. The carrier frequency has been set on-resonance of all the reported ^{27}Al NMR spectra.

(37) Schnell, I. *Prog. Nucl. Magn. Reson. Spectrosc.* **2004**, *45*, 145.

Results and Discussion

Isolation of MIL-121. In the Al−H_4btec-H_2O system, the crystallization of three distinct phases is observed (Figure 3). They are MIL-118A ($Al_2(OH)_2(H_2O)_2$[btec]), MIL-120 ($Al_4(OH)_8$[btec]·4.8−5H_2O), and the title compound MIL-121 (Al(OH)[H_2btec]·(guest) (guest = H_2O, H_4btec). We analyzed this particular chemical system at 180 °C because of technical restrictions of the high-throughput setup although the typical synthesis conditions were given at 210 °C for the different phases. In fact, we observed that the temperature difference did not affect drastically the phase domains but rather the crystal growth kinetics. It was found that higher temperature of the hydrothermal reactions favored a better crystallization, which made easier the crystal structure determination by either single-crystal microdiffraction or powder diffraction. The variation of the molar composition Al/H_4btec/H_2O gives rise to the observation of two main phase domains for which MIL-121 appears in concentrated Al solutions whereas MIL-118A crystallized in a narrower domain in diluted Al solutions. Between them, we observed a mixture of these two phases with the progressive decreasing of the MIL-121 amount when the Al dilution increases. The third phase, MIL-120, is formed at higher pH, and similar synthesis experiments were carried out in the presence of NaOH with a given [Al]/[OH] ratio of 1.6. In this condition, the existence domain of MIL-121 is much smaller, and the decreasing of Al concentration led to different mixtures including small amounts of MIL-118A, MIL-121, and the third solid MIL-120. The latter is obtained as a pure form for diluted Al systems. The formation of the aluminum pyromellitates is influenced by the pH value of the hydrothermal reaction, which gives rise to the formation of MIL-118A (acidic) or MIL-120 (basic) in diluted Al solutions, as well as the reactants concentration with the crystallization of MIL-121 for relatively high concentrated Al solutions.

Structure Description. The MIL-121 structure is built up from the connection of infinite chains of $AlO_4(OH)_2$ octahedra with the pyromellitate ligand (Figure 4). Aluminum is 6-fold coordinated with four carboxyl oxygen atoms and two remaining oxygen atoms (hydroxo groups) in *trans* position in the octahedral surrounding (with typical Al−O bonding of 1.867(2)−1.905(4) Å). The latter species connect to each other two adjacent aluminum cations to generate straight inorganic chains running along

(38) Massiot, D.; Fayon, F.; Capron, M.; King, I.; Le Calve, S.; Alonso, B.; Durand, J. O.; Bujoli, B.; Gan, Z. H.; Hoatson, G. *Magn. Reson. Chem.* **2002**, *40*, 70.

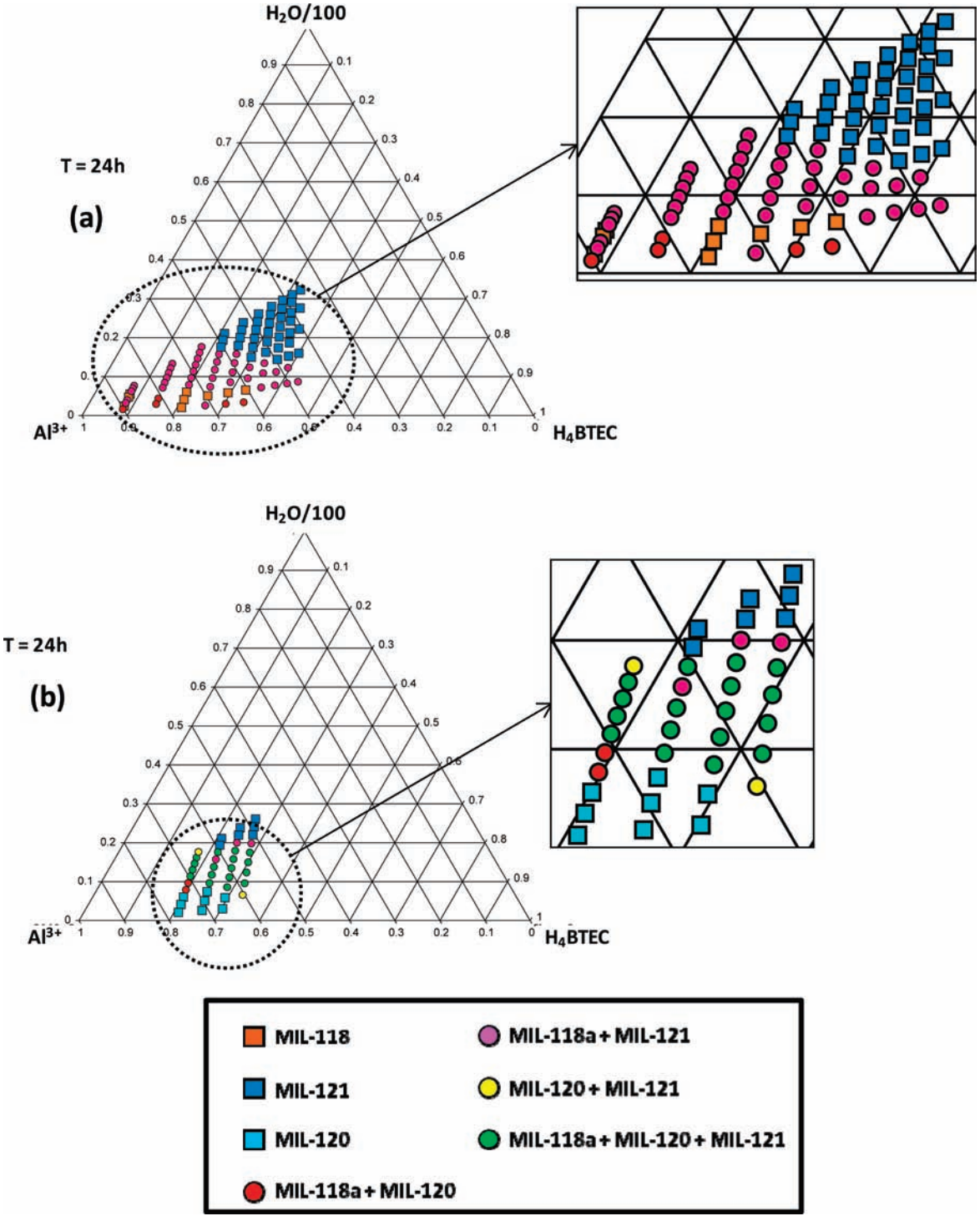

Figure 3. Ternary phase diagrams of the chemical systems (a) Al−H_4btec-H_2O and (b) Al−H_4btec-H_2O-NaOH (with a fixed molar concentration ratio of [NaOH]/[Al] = 1.3), indicating the existence domains of the three aluminum pyromellitates MIL-118A, MIL-120, and MIL-121.

the *c* axis (Figure 5). This specific building brick is now well-known and has been observed in many MOF-type aluminum-based carboxylates displaying 3D networks.[33,39−43] These chains are linked via the carboxylate groups of the pyromellitate ligand, which display a *syn-syn* bidentate bridging mode between two adjacent aluminum atoms. Only two carboxylate arms (1,4 positions) of the pyromellitate play the role of linker while the two remaining (2,5 positions) are non-linking and remain in protonated form. Infrared spectroscopy (see Supporting Information) confirms

(39) Loiseau, T.; Serre, C.; Huguenard, C.; Fink, G.; Taulelle, F.; Henry, M.; Bataille, T.; Férey, G. *Chem.—Eur. J.* **2004**, *10*, 1373.
(40) Loiseau, T.; Mellot-Draznieks, C.; Muguerra, H.; Férey, G.; Haouas, M.; Taulelle, F. *C. R. Chimie* **2005**, *8*, 765.
(41) Senkovska, I.; Hoffmann, F.; Fröba, M.; Getzschmann, J.; Böhlmann, W.; Kaskel, S. *Microporous Mesoporous Mater.* **2009**, *122*, 93.
(42) Comotti, A.; Bracco, S.; Sozzani, O.; Horike, S.; Matsuda, R.; Chen, J.; Takata, M.; Kubota, Y.; Kitagawa, S. *J. Am. Chem. Soc.* **2008**, *130*, 13664.
(43) Volkringer, C.; Loiseau, T.; Guillou, N.; Férey, G.; Elkaïm, E. *Solid State Sci.* **2009**, *11*, 1507.

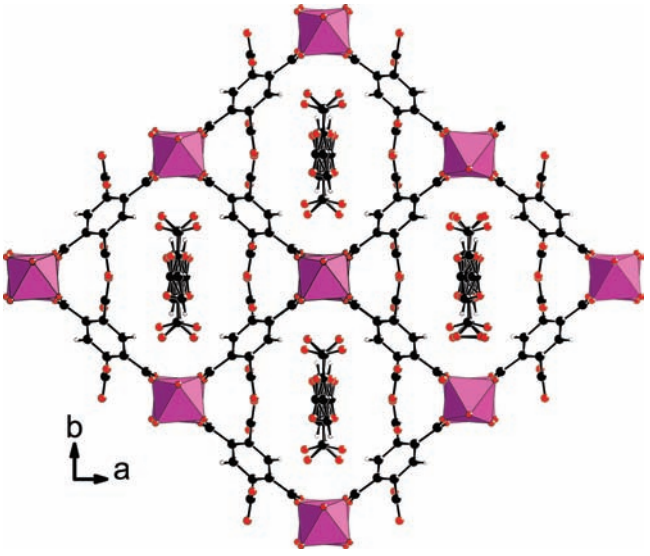

Figure 4. View of the structure of MIL-121_as along the *c* axis, showing the channels encapsulating disordered free water and pyromellitic acid molecules. Purple octahedra, $AlO_4(OH)_2$; black circles, carbon; red circles, oxygen; open circles, hydrogen.

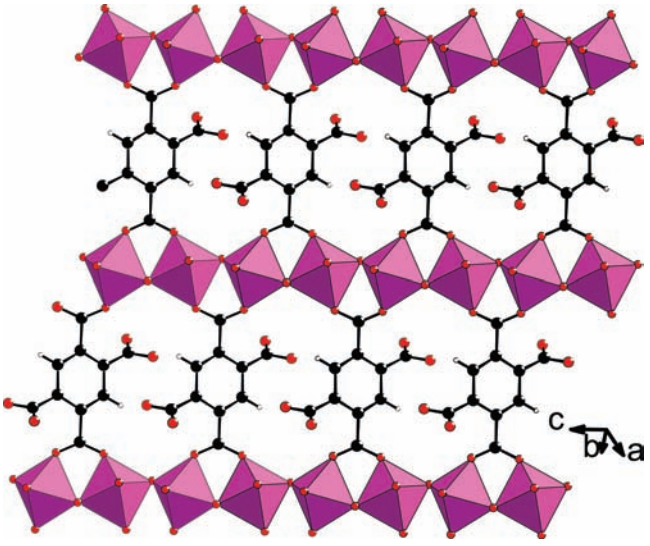

Figure 5. View of the structure of MIL-121 showing the trans-connected chains of $AlO_4(OH)_2$ octahedra linked to each other through the partly protonated pyromellitate ligands. Purple octahedra, $AlO_4(OH)_2$; black circles, carbon; red circles, oxygen; open circles, hydrogen.

this last point since the band observed at 1815 cm^{-1} ($\nu_{C=O}$) is assigned to the non-coordinating −COOH function. The organic molecule adopts a configuration μ_4-η_1:η_1:η_1:η_1. This type of connection is reminiscent of that occurring for the 1,4-benzenedicarboxylate linker found in the aluminum terephthalate MIL-53.[39] Similar arrangement has also been reported with longer molecules such as 2,6-naphthalenedicarboxylate,[40,41] 4,4′-biphenyldicarboxylate,[41] or 1,4-naphthalenedicarboxylate.[42] Therefore, the channels delimited by the inorganic chains and ligands (free aperture: 8.7 × 5.7 Å) are developed along the *c* axis, with an open configuration close to that observed in the high temperature form of the parent MIL-53 phase. The cell volumes of the two solids reflect well this analogy (MIL-121_as: 1459.25 $Å^3$; MIL-53_ht: 1411.95 $Å^3$). In MIL-53, a pore volume change was observed depending on the temperature or the nature of the encapsulated species within the channels. This means that MIL-121 exhibits an open form because of the steric hindrance of the non-bonded carboxylate groups of the pyromellitate linker. The latter occupy specific positions to generate an infinite weak hydrogen bonding network between two $-CO_2H$ species (O···O = 3.336(8) Å) from two adjacent organic linkers along the channel axis, in the (*b*,*c*) plane. It is interesting to notice that this configuration differs if one considers another cation such as iron(III) in MIL-82.[24,25] In the latter, the structural topology is identical except the position of the free carboxylates groups, which are located with a 180° rotation in the aromatic cycle. It results in a closed form with a smaller cell volume (1096 $Å^3$), because of the hydrogen bond interactions between the $-CO_2H$ groups, which are placed toward the center of the tunnels, where water molecules are trapped. In MIL-121, the $R-CO_2H$ groups are located along the inorganic chains axis, releasing free space in the center of the channels. Such a change of open/closed forms as a function of the cation nature was previously well described during the dehydration process of the hydrated forms of MIL-53(Al, Fe). While an open form is obtained upon water removal with aluminum (or chromium[44]), the iron-based compound still remains in closed form.[45] For the compounds MIL-121/-82, the driving force for the open/closed forms is clearly controlled by the positions of the non-coordinated −COOH groups, which will direct the hydrogen networks and induce the open/closed forms. For other reasons, it is noticeable to have similar behavior between aluminum and iron with different organic linkers.[46] Within the channels of MIL-121 are found unreacted pyromellitic acid or water species, which are disordered on several positions. The presence of such trapped molecules in MIL-121_as is further confirmed by other techniques such as IR, and NMR spectroscopy as well as TGA measurements.

Infrared Spectroscopy. The IR spectrum of MIL-121_as exhibits several bands assigned to the vibrational modes of carboxylates (see Supporting Information). The bands at 3018, 2659, and 2526 cm^{-1} are assigned to the ν_{CO-H} modes of free −COOH functions.[47] These vibrations indicate the presence of hydrogen bonds with water (ν_{O-H} at 3445 cm^{-1}) and carboxylic acids. We assume that these last species can correspond to non-bonded −COOH groups from pyromellitic acids trapped into the pores and non-coordinating −COOH groups from the framework. In the 1600−1800 cm^{-1} range we can differentiate the non-bonded −COOH groups and those connected to aluminum. The peak at 1601 cm^{-1} corresponds to the stretching vibration of carboxylate coordinated to the cation, whereas the vibrations at 1739 and 1713 cm^{-1} are assigned to non-coordinated functions. For these two last bands, we are not able to assign the one coming from non-coordinating −COOH functions from the framework and those from trapped carboxylic acids. The peak observed at 3618 cm^{-1} corresponds to the ν_{O-H} vibration of the μ_2-hydroxo group, bridging aluminum

(44) Millange, F.; Serre, C.; Férey, G. *Chem. Commun.* **2002**, 822.
(45) Millange, F.; Guillou, N.; Walton, R. I.; Grenèche, J. M.; Margiolaki, I.; Férey, G. *Chem. Commun.* **2008**, 4732.
(46) Volkringer, C.; Loiseau, T.; Guillou, N.; Férey, G.; Elkaïm, E.; Vimont, A. *Dalton Trans.* **2009**, 2241.
(47) Pretsch, E.; Buhlmann, P.; Affolter, C. *Structure Determination of Organic Compounds*; Springer-Verlag: Berlin, Heidelberg, 2000.

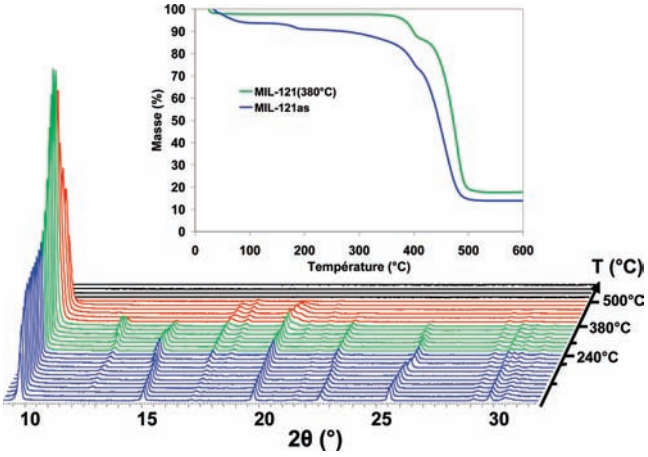

Figure 6. Thermogravimetric analysis curves (under O_2, 1 °C/min) of the aluminum pyromellitate MIL-121as and the activated MIL-121 form (after heating at 380 °C for 5 h) and the evolution of the XRD patterns of MIL-121as as a function of temperature (λ_{Co} = 1.7903 Å, under air).

cations (Al−OH−Al). This value is in agreement with those observed with MIL-53 (Al).[46]

To complete this attribution, IR data of the activated MIL-121_ht was collected. MIL-121 spectra still show the vibration corresponding to connected carboxylate functions, and we deduce that the additional sharp band at 1815 cm^{-1} characterized the non-coordinating carboxylates of the framework. The efficiency of the activation is highlighted by the absence of bands previously described at around 2500 and 1700 cm^{-1}.

Thermal Behavior. The thermal behavior of MIL-121 was characterized by thermogravimetric analyses and X-ray thermodiffraction (Figure 6). The TG curve of the activated MIL-121_ht solid exhibits two events. The first one is visible from room temperature up to 70 °C and corresponds to trapped water molecules (observed weight loss of 2.3%, equivalent to 0.4 H_2O/Al). After a plateau up to 380 °C, the decomposition of the organic ligand occurs in two steps. The first weight loss between 380 and 410 °C could be assigned to the departure of two CO_2 molecules from the non-coordinating −COOH groups (obs.: 10%, calc.: 7.6%). The second step between 410 and 520 °C is attributed to the decomposition of the ligand (obs.: 69.3%; calc.: 71.5%). The final residue (obs.: 17.6%) is a white powder and corresponds to aluminum oxide Al_2O_3 (calc.: 16.8%). The TG curve of the as-synthesized product (MIL-121_as) slightly differs since a continuous weight loss is observed between room temperature and 360 °C. The first step between room temperature and 200 °C is assigned to the departure of trapped water molecules (obs.: 7.2% or 1.5 H_2O/Al). From 200 up to 360 °C, the second weight loss could be attributed to the removal of the free pyromellitic acid (encapsulated within the channel), and this would correspond to 0.1 H_4btec/Al (obs.: 6.1%). This step is not observed for the activated MIL-121_ht form, for which the trapped organic species have been removed. The total decomposition of the organic ligand occurs between 380 and 520 °C (obs.: 70.5%; calc.: 68.6%). The final residue (obs.: 14%) is a white powder and corresponds to aluminum oxide Al_2O_3 (calc.: 14.6%). One can notice that the content of the encapsulated species (H_4btec, H_2O) differs from those obtained from the powder XRD data analysis. The latter gave a chemical formula Al(OH)-(H_2btec)·0.27H_4btec·0.19H_2O, while TGA gives Al(OH)-(H_2btec)·0.1H_4btec·1.5H_2O. The latter composition is close to the elementary chemical analysis which gave: Al: obs: 6.84% ; calc: 7.74% ; C: obs: 36.13% ; calc: 37.88% ; H: obs: 2.00% ; calc: 2.46% for MIL-121_as. This difference may come from the difficulties to measure the exact amount of adsorbed water in porous matrixes, since this value is sensitive to ambient air moisture. This varies according to the situation of the experiment measurement (TG cell in a laboratory or glass capillary under high flux X-ray from synchrotron radiation). Moreover, there are still some difficulties to accurately locate disordered molecules trapped within one-dimensional (1D) channels of porous frameworks by XRD.

The X-ray thermodiffraction experiment carried out on the as-synthesized MIL-121_as phase indicates that its framework is not very flexible. Indeed, only very small shifts of the diffraction lines toward lower or higher angles occur at about 200 °C, indicating a slight modification of the unit cell parameters. The structure still remains in an open form, whereas a transition "closed/open channel" was reported in the parent MIL-53[39] compound. Nevertheless, an increase of the Bragg peaks intensity at low angles is observed, which would reflect the removal of the inserted species within the channels, especially the encapsulated pyromellitic acid and water molecules. After 380 °C, there is a continuous decrease of the Bragg peaks intensity, and at 500 °C, no signal is observed, indicating the structural collapse and the formation of an amorphous product. The different series of patterns clearly shows that MIL-121 is thermally stable up to 380 °C, which is a lower value than that of the parent MIL-53 compounds, involving the terephthalate anions (up to 500 °C[39]) or aminoterephthalate anions (up to 410 °C[17]) as linkers.

The porosity of the activated compound of MIL-121 was characterized by the Brunauer−Emmett−Teller (BET) method with the adsorption of liquid nitrogen at 77 K. The BET and Langmuir specific surface areas were 162(6) $m^2\ g^{-1}$ and 244(1) $m^2\ g^{-1}$, respectively. These values are much lower than the ones determined for the parent compound MIL-53 involving 1,4-benzenedicarboxylate linker[39] (BET: 1140 $m^2\ g^{-1}$). The decrease of the specific surface area is due to the steric hindrance of the free non-coordinated −COOH groups within the channels, which reduce the access of other guest molecules.

Solid State NMR. The two samples of MIL-121_as and MIL-121_ht have been analyzed by solid-state NMR. The purpose of the study was to clarify the relation between the diffraction analysis of the periodic lattice and the actual crystal structure sensed by NMR. The second goal of the study was to compare the as-synthesized compound with the activated one. In the as-synthesized compound one may always have a fraction of the crystal, which might not be fully periodic, that NMR can contribute the most to the crystal structure analysis. The synthesis has been carried out with very few components, namely, water, aluminum nitrate, and pyromellitic acid, indicating for an NMR analysis that the ^{27}Al, ^{13}C, and ^{1}H nuclei are expected in the solid (nitrate anions were not revealed from chemical analysis). Therefore, 1D ^{1}H MAS, $^{13}C\{^{1}H\}$ CPMAS, and ^{27}Al MAS experiments have been acquired, as well as 2D ^{1}H-^{1}H DQ-SQ, ^{1}H-^{1}H RFDR, and $^{27}Al\{^{1}H\}$ CPHETCOR.

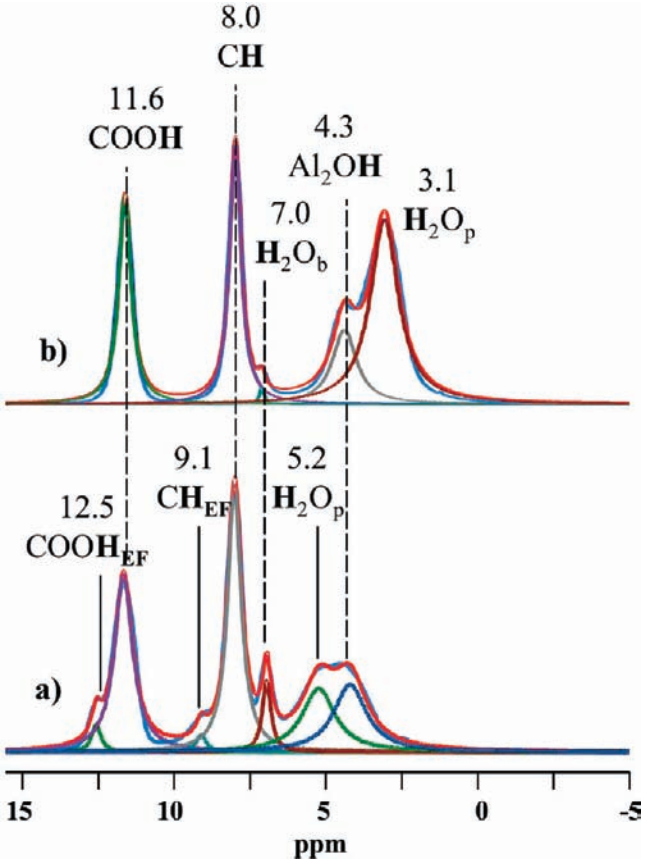

Figure 7. ^{1}H MAS spectra of (a) MIL-121_as, and (b) MIL-121_ht. Signal area ratios are respectively as follows: 41 (3.1): 14 (4.3): 1 (7.0): 24 (8.0): 20 (11.6) for spectrum (a), and: 18 (4.3): 17 (5.2): 5 (7.0): 30 (8.0): 1 (9.1): 27 (11.6): 2 (12.5) for spectrum (b). All spectra were recorded at 500 MHz and spinning rate 30 kHz.

Figure 7 shows the ^{1}H NMR spectra of the two forms of MIL-121. In MIL-121_as, four main signals at 11.6, 8.0, 5.2, and 4.4 ppm with three additional minor signals at 12.5, 9.1, and 6.9 ppm are observed. As the main signal at 8.0 ppm can unambiguously be assigned to the aromatic C**H**, they can also be used to normalize the intensities of other peaks relatively to framework H_2btec. The main signal at 11.6 ppm is assigned to protonated carboxylic groups COO**H**, confirming that non-bonding carboxylic groups are present per framework H_2btec species. Among the two remaining major signals, the signal at 4.2 ppm is the bridging hydroxyl group between aluminum atoms Al_2O**H** (or O**H**), and the second major signals at 5.2 ppm is assigned to water within the pores, $\mathbf{H_2O_p}$.[39] The minor signals at 12.5 ppm and 9.1 ppm are respectively the carboxylic acid and aromatic protons of the extra-framework H_4btec, $\mathrm{COOH_{EF}}$ and $\mathrm{CH_{EF}}$. The 6.9 ppm signal can therefore only be some water, not exchangeable with the water molecules within the pores, and strongly associated to carboxylic acid groups because of its high value of chemical shift $\mathbf{H_2O_b}$. Both locations of some water in the infinite hydrogen bonding network, or directly hydrogen bonding extra-framework pyromellitic acid groups lead to non-integer stoichiometric amounts for these sites and no exchange with $\mathbf{H_2O_p}$. In MIL121_ht, four main signals at 11.5, 8.0, 4.4, and 3.1 ppm are observed with one additional minor signal at 7.1 ppm. The 11.5 and 8.0 ppm signals are assigned to the framework carboxylic protonated groups and the aromatic protons as in the case of MIL-121_as. The 4.4 ppm signal is assigned to the bridging hydroxyl groups O**H** and the 3.1 ppm to the remaining water in the pores, $\mathbf{H_2O_p}$. Water is known to have its chemical shift highly dependent on its environment and its concentration. Its relatively large intensity indicates that the activated compound became somehow more hydrophilic than the as-synthesized compound. Finally, the 7.1 ppm signal is assigned to water strongly hydrogen bonded to COOH groups. As the activation has eliminated the extra-framework pyromellitic acids, the water can only be located in defects of the infinite hydrogen-bonding network of the framework, blocking its chemical exchange with the remaining water.

These assignments based upon qualitative reasoning need to be validated by additional experiments or information. Three signals appear to belong to the framework; they are the peaks at 11.5 and 8.0 ppm from H_2btec, and those at 4.4 or 4.2 ppm from hydroxyl groups. They are definitely present in both as-synthesized and activated samples, and should exhibit a population ratio of 2 H: 2 H: 1 H corresponding to the btec aromatic C**H**, COO**H** and Al_2−O**H** (or O**H**) groups. The experimental ratio observed for both the as-synthesized and activated samples is 1.7: 2.0: 1.2. Though the total amount of protons 4.9 is approximately the expected ratio of 5.0, a slight underestimation of COO**H** sites and a small overestimation of the O**H** sites are observed. One may expect such a small transfer of proton mediated by the nearby water. Actually H_2O is less acidic than the carboxylic acid groups and more acidic than the bridging hydroxyl group. Depending on the exact p*K* values of both groups within the crystals some transfer may take place between the most acidic and the most basic sites.

The extra-framework pyromellitic acid molecules are observed in both ^{1}H MAS and ^{1}H→^{13}C CP MAS spectra. In the first spectrum COO**H** and C**H** signals are observed at 12.5 and 9.1 ppm in an approximately 2:1 ratio. In the second ^{13}C spectrum (see Supporting Information), the **C**OOH, aromatic quaternary **C**-COOH and aromatic **C**H appear respectively in the chemical shift ranges of 175−165, 136−134, and 130 ppm. Moreover, ^{1}H→^{13}C CP MAS spectrum of MIL-121_as exhibits besides the intense signals of the carboxylic framework H_2btec, at about 172−173 ppm, small peaks at 165.0, 169.0, and 177.0 ppm of $\mathbf{C}\mathrm{OOH_{EF}}$ assigned to extra-framework H_4btec. This multiplicity indicates most probably a lower symmetry for the extra-framework H_4btec carboxylic sites than for the framework H_2btec. The $\mathbf{C}\mathrm{H_{EF}}$ signal at 127.7 ppm is the only aromatic signal of the extra framework H_4btec that can be distinguished from the framework H_2btec aromatic signals. One can therefore evaluate the amount of extra-framework H_4btec in MIL-121_as approximately 0.07 H_4btec per framework H_2btec or per Al according to quantitative ^{1}H NMR spectrum. The extra-framework H_4btec are removed by activation. These observations are fully consistent with IR and TGA results. The latter gave the same order of magnitude of encapsulated species.

On the ^{1}H side only the assignment of two signals per spectrum remain to be validated: the signal at 5.2 ppm observed in the ^{1}H spectrum of MIL-121_as, and 3.1 ppm for MIL-121_ht, and for both compounds the signal at

6.9−7.1 ppm. The two first signals are assigned to water molecules and have a pronounced chemical shift difference arising for MIL-121_as from the crystallization water and for the activated one by its spontaneous rehydration. The water species in the case of the as-synthesized and activated sample have a strongly different interaction with extra-framework H_4btec or directly with the framework H_2btec that already have their hydrogen bonds saturated within the framework. This is the origin of the strong chemical shift difference. The amount of water present as guest molecules was found to be $0.6H_2O$ per framework Al(OH)[H_2btec] unit before activation and became $1.7H_2O$ per Al after removal of extra-framework organic species, with the sample stored in ambient air. The presence of the extra-framework H_4btec introduces some hydrophobicity with the aromatic rings, and some volume occupancy in the material. Activation by thermal treatment improves the access of water to the pores by freeing some volume and removing hydrophobicity. 2D ^{1}H-^{1}H experiments have been used to clarify the water situation. First, a double quantum to single quantum correlation (DQ-SQ) using a BABA excitation and reconversion of dipolar coupling reintroduction, and second a single quantum-single quantum (SQ-SQ) RFDR sequence were acquired on sample MIL-121_ht to gain more information on the assignment and the nature of interaction between the different protons. These experiments are complementary, where the 2D DQ-SQ spectrum provides short-range interaction, whereas the 2D SQ-SQ RFDR spectrum provides much longer range interaction. The DQ-SQ experiment has a unique characteristic, by showing evidence of dipolar coupling occurring between crystallographically identical sites whereas RFDR experiments sense the dipolar couplings to a much longer distance range. Figure 8 shows 2D BABA contour plots of MIL-121_ht acquired with two different mixing times. The connectivities between distinct proton signals are shown as horizontal lines in Figure 8. The strong correlations between signals at bridging O**H**, C**H**, and COO**H** ppm indicate clearly their presence in vicinity to each other. It confirms their assignment to framework protons of the bridging hydroxide groups and H_2btec of the network. The small signal assigned to $\mathbf{H_2O_b}$ at 7.1 ppm correlates with the C**H** of framework H_2btec resonance at 7.9 ppm indicating that the corresponding species is at a short distance of the framework organic linker. This signal, however, does not show any correlation with O**H** groups resonance at 4.3 ppm, indicating a longer distance to O**H** groups. The signal at 2.4−2.9 ppm assigned to $\mathbf{H_2O_p}$, present only an autocorrelation, appears to be very weak in the experiment with short mixing time (133 μs), and its intensity increases only slightly with longer mixing time (266 μs). This result is consistent with the existence of water clusters weakly interacting with the host material. This weak intensity reflects also a small residual dipolar interaction, indicating some water mobility of at least rotational origin. Except from the self-correlated sites, the same results are obtained with the RFDR spectrum recorded with 266 μs mixing time (Figure 9a) exhibiting the same correlations previously seen in the DQ experiments. RFDR correlations for long mixing time (2.66 ms) shown in Figure 9b, involve the water signal of $\mathbf{H_2O_p}$ at 3 ppm with the three signals belonging to the framework indicating a long distance

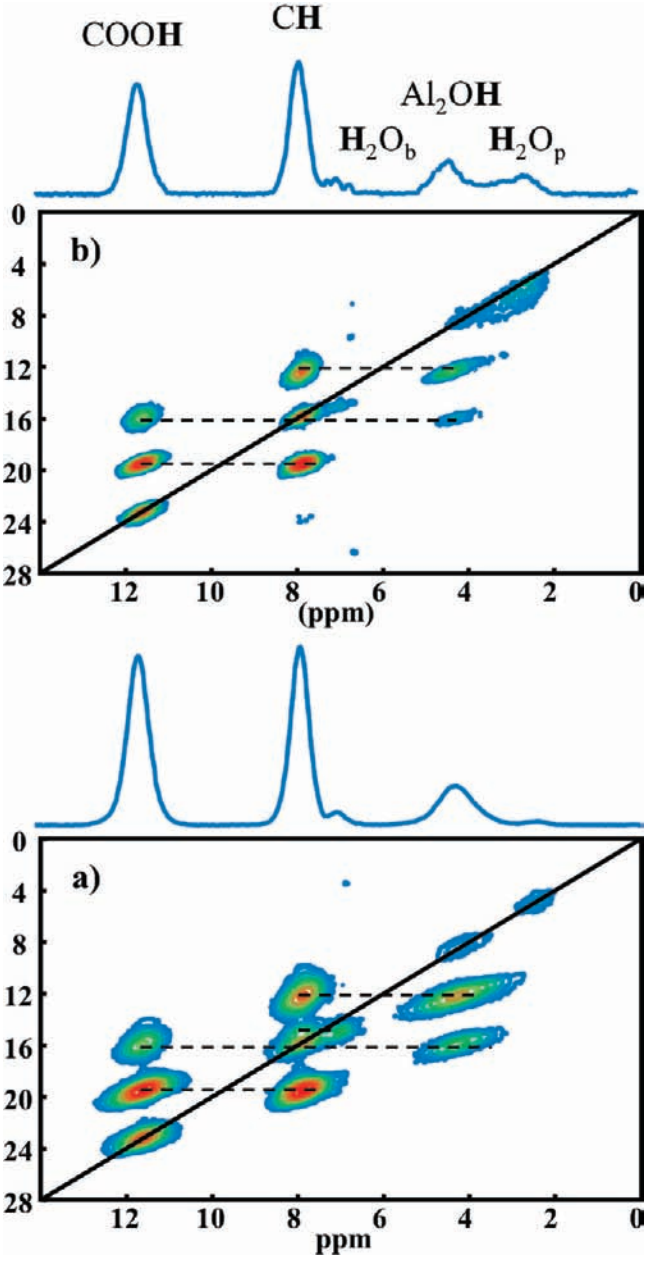

Figure 8. 2D ^{1}H-^{1}H back-to-back spectra of MIL-121_ht acquired with mixing time of (a) 133 μs, and (b) 266 μs. All spectra were recorded with a spinning speed of 30 kHz and four rotor periods for excitation and reconversion.

between water and the framework. The correlation between $\mathbf{H_2O_b}$ at 7 ppm and COO**H** at 11.7 ppm and C**H** at 7.9 ppm signals is also observed in this experiment, revealing a shorter distance between $\mathbf{H_2O_b}$ and C**H** than with COO**H**. This is consistent with having $\mathbf{H_2O_b}$ in the infinite hydrogen bonding network, a position that shares this geometrical situation.

Concerning the framework, aluminum can probe the consistency between NMR and diffraction nicely. ^{27}Al MAS NMR spectra, (Figure 10), showed a single signal for MIL-121_as and MIL-121_ht. The quadrupolar parameters for both phases are very close but show that a slight difference in cell parameters is present, measured by a small but measurable difference in the C_Q and η_Q value for both phases. Indeed, an increase of C_Q from about 8 to

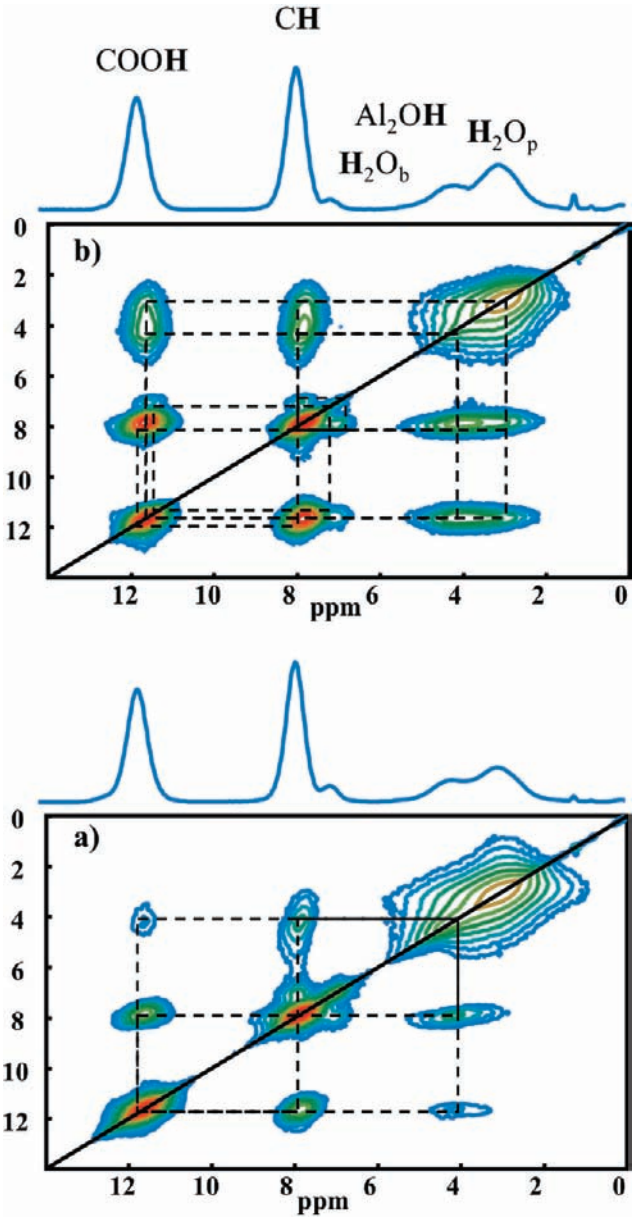

Figure 9. 2D ^{1}H-^{1}H RFDR spectra of MIL-121_ht acquired with mixing time of (a) 266 μs, and (b) 2.66 ms.. All spectra were recorded with a spinning speed of 30 kHz.

9 MHz is observed after thermal treatment for activation. The MQMAS spectrum of MIL-121_ht (see Supporting Information) confirmed that only one resonance is present. This slight variation of quadrupolar parameters contrasts with MIL-53, for which, upon rehydration, the compound undergoes a closing of the pores. The MQMAS spectrum can be used additionally to determine precisely the isotropic chemical shift and the quadrupolar parameters. Both signals are resonating at around 1−3 ppm, typical values for 6-fold coordinated aluminum with oxygen atoms in first sphere of coordination. These results are fully consistent with the crystallographic data for which an unique octahedrally coordinated Al site was found in both MIL-121. However, this may indicate that the removal of residual organic extra-framework species induces a slight change of the unit cell parameters. Further insights on assignment and interaction of the different species with the inorganic

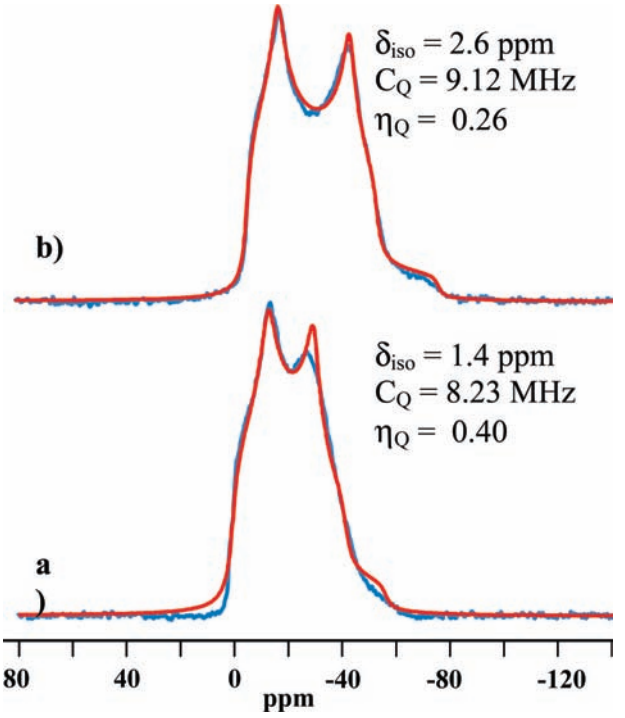

Figure 10. ^{27}Al MAS spectra of (a) MIL-121_as, and (b) MIL-121_ht. All spectra were recorded at 130 MHz and spinning rate 30 kHz.

part of the network are provided by the ^{27}Al{^{1}H} CPHETCOR MAS experiment. Figure 11 shows two 2D spectra obtained with two different contact times. At short contact time (0.1 ms), a unique correlation was observed between the ^{27}Al signal and the ^{1}H resonance of O**H** at 4.2 ppm. This proves definitively the assignment of the 4.2−4.4 ppm in ^{1}H spectra to Al_2−O**H** groups because these protons should be the one exhibiting the strongest heteronuclear dipolar interaction with ^{27}Al nucleus. At longer contact time (1.5 ms), the same ^{27}Al signal showed now additional correlations with proton signals of C**H** at 7.9 and COO**H** at 11.8 ppm as a result of long-range interaction with the framework protons located on the H_2btec moieties. This is consistent with the assignment of these protons to respectively aromatic and carboxylic acid protons of the framework. On the other hand, no correlation has been observed with the proton signal of $\mathbf{H_2O_p}$ at about 3 ppm indicating no efficient CP transfer from these protons. This confirms the weakness of the dipolar interaction of water clusters with framework Al because of longer distances and some mobility of the corresponding species. The overall results points to weakly adsorbed water clusters in the pores. The NMR results can be summed up as providing the following picture for MIL-121 compounds. The framework description provided by diffraction is confirmed by NMR, but one can add some additional points. First, some protons are transferred from the sublattice of COOH groups from the framework H_2btec to the Al_2−O**H**. Second, some water molecules are trapped in the infinite hydrogen bonding chains occurring between COOH of the framework H_2btec. Third, the extra-framework H_4btec in MIL-121_as are forming with water a structured sublattice that collapses during activation. Fourth, when spontaneous rehydration of the activated MIL-121_ht occurs, structured water clusters are formed in the pore of the compound. At contrast to what

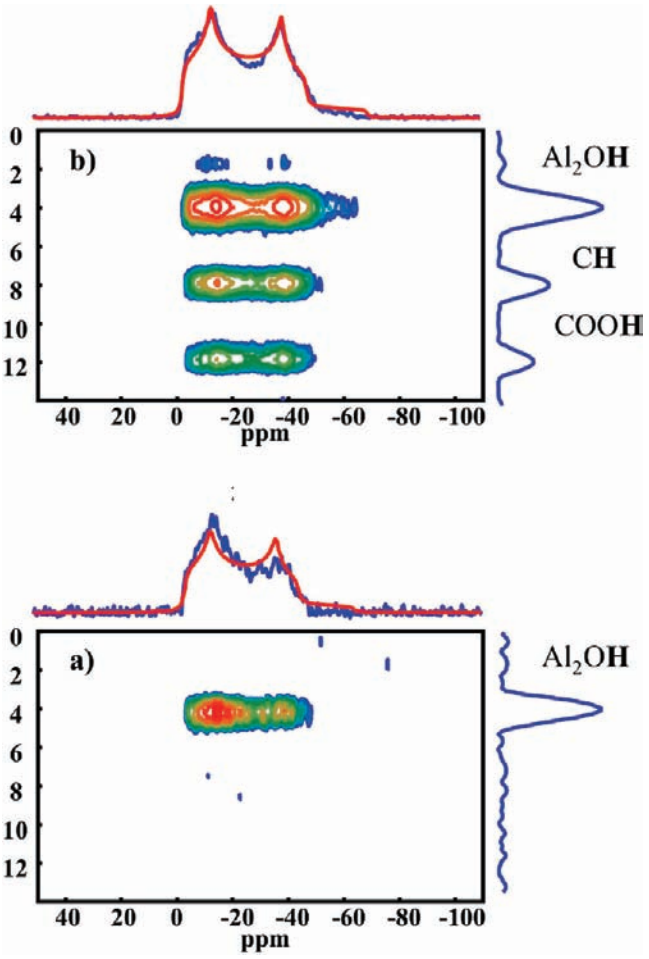

Figure 11. 2D $^{27}Al\{^{1}H\}$ CP HETCOR MAS spectra of MIL-121_ht recorded with (a) 0.1 ms and (b) 1.5 ms contact times. All spectra were recorded with a spinning speed of 30 kHz.

occurs for MIL-53, the rehydration of the structure leaves the pores in their open state, as also sensed by ^{27}Al NMR.

Conclusion

In this paper we have described the synthesis and characterization of a new porous aluminum-based MOF called MIL-121 displaying two free non-coordinating carboxylic functions per ligand. For this study, we chose high-throughput aided synthesis to establish the phase domain of this solid in the system aluminum-pyromellitate-NaOH-water together with the two other phases MIL-118 and MIL-120. This tool enabled the isolation of each compound and also highlighted the influence of the pH on the formation of the different frameworks. Regarding the connectivity of aluminum in the inorganic subnetwork, low pH favors a connection via μ_2-hydroxo corner (MIL-118 and MIL-121) of AlO_6 octahedra whereas for higher values of pH, the aluminum-centered octahedra are linked to each other with common edge corresponding to two μ_2-hydroxo groups (MIL-120). On the organic part, the increase of the starting pH value induces a constant augmentation of the number of coordinating oxygen atoms per pyromellitate ligand. For MIL-121, MIL-118, and MIL-120 respectively 4, 6, and 8 carboxyl oxygen atoms are connected to aluminum cations. These observations are presented in Figure 12.

MOF-type Aluminum Pyromellitate	Organic ligand configuration	Inorganic sub-network configuration	Starting pH value
MIL-120			12.2
MIL-118			2
MIL-121			1.4

Figure 12. Influence of pH related to the formation of MOF-type aluminum pyromellitate frameworks.

Acknowledgment. the authors would like to thank Dr Eric Leroy and Dr Michel Latroche (ICMPE, Thiais, France) for their assistance for the SEM images.

Supporting Information Available: Further details are given in Figures S1−S5. This material is available free of charge via the Internet at http://pubs.acs.org.